

Supporting Information (SI) File

BMIM-BF₄ RTIL: Synthesis, Characterization and Performance Evaluation for Electrochemical CO₂ Reduction to CO over Sn and MoSi₂ Cathodes

Ibram Ganesh*

*Centre of Excellence for Artificial Photosynthesis,
International Advanced Research Centre for Powder Metallurgy and New Materials (ARCI),
Balapur Post, Hyderabad – 500 005, Telangana, India.*

(*E-mail: ibramganesh@arci.res.in; dribramganesh@gmail.com; fax: +91-40-24442699)

Table of contents

1.	Supporting information (SI) schemes, and figures captions	S2-S3
2.	Preparation procedure of 0.5 M sodium phosphate (NaPi) (pH-7.4) buffer solution	S4-S5
3.	Quantitative estimation of CO and H ₂ gases formed in electrochemical CO ₂ reduction (ECR) reaction using gas-chromatography mass-spectrometry (GC-MS) technique	S5-S7
4.	Determination of Faradaic efficiency (FE)	S7
5.	Determination of number of moles of CO and H ₂ gas-mixture formed in the ECR reaction in CPBE experiments	S8
6.	Calculation of turnover frequency (TOF)	S8
7.	Calculation of yield	S9
8.	Tafel slopes generation	S9
9.	Calibration of reference electrode	S9
10.	Supporting information Schemes, and Figures	S10-S23
	References	S24

1. Supporting information (SI) schemes, and figures captions

- Scheme S1. A schematic diagram showing a plausible reaction mechanism proposed by Wang *et al.* [9], that is believed to take place in an imidazolium based RTIL mediated ECR reaction to form CO in the presence of protons (H^+) derived from water on the surface of an inert metal cathode.
- Figure S1. XRD pattern of NaBr formed as a byproduct during synthesis of bmim[BF₄] RTIL from bmim[Br] and NaBF₄ *via* metathesis reaction performed at room temperature in water medium along with ICDD file # 00-005-0591 assigned for NaBr compound.
- Figure S2. A digital photograph showing the continuous liquid-liquid extraction apparatus employed for separating bmim[BF₄] RTIL from NaBr salt from the reaction mixture solution.
- Figure S3. CV profile generated while calibrating Ag/Ag^I (0.01M) reference electrode in Ar saturated and blanketed solution of 20 mL MeCN + 200 mM n-Bu₄NPF₆ + 5 mM Ferrocene at a scan rate of 20 mV/s over Pt working (WE) and counter electrodes (CE).
- Figure S4 (a). ¹H-NMR spectrum of bmim[Br] RTIL synthesized in this study (refer Table 2).
- Figure S4 (b). ¹³C-NMR (125 MHz, CDCl₃ + DMSO) spectrum of bmim[Br] compound synthesized in this study (refer Table 2).
- Figure S5 (a). ¹H-NMR of bmim[BF₄] RTIL prepared in this study (refer Table 2).
- Figure S5 (b). ¹³C-NMR (125 MHz, CDCl₃ + DMSO) of bmim[BF₄] RTIL prepared in this study (refer Table 2).
- Figure S6 (a). ¹H NMR (400 MHz, CDCl₃) spectrum of bmim[BF₄] (≥97.0%, 91508-5G) RTIL procured from Aldrich, USA (refer Table 2).
- Figure S6 (b). ¹³C-NMR spectrum of bmim[BF₄] (≥97.0%, 91508-5G) RTIL procured from Aldrich, USA (refer Table 2).
- Figure S7. (a) Gas chromatograph (GC) profiles gases formed in cathodic compartment during a CPBE experiment performed as per reaction conditions given 1st and 3rd

rows of Table 3, respectively; and (b) the response factors of H₂ and CO gases by thermal conductivity detector (TCD).

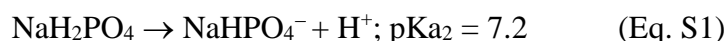
Figure S8. XRD pattern of a white precipitate *in situ* formed in the cathodic compartment during CPBE experiment conducted as per the reaction conditions given in the 3rd row of Table 3. All the major XRD peaks exhibited by this white precipitate are matching with those lines of NaHCO₃ published in ICDD File # 00-003-0653.

Figure S9 (a). ¹H NMR (400 MHz, CDCl₃) spectrum of concentrated catholyte solution of CPBE experiment performed as per the reaction conditions given in 3rd row of Table 3: δ (ppm) = For bmim[BF₄]: 0.95 (3H, m, but-CH₃; C₉), 1.36 (2H, m, but-CH₂; C₈), 1.87 (2H, m, but-CH₂; C₇), 3.97 (3H, s, N-CH₃; C₁₀), 4.23 (2H, t, but-N-CH₂; C₆), 7.43 (1H, s, imidazole ring-N-CH-; C₄), 7.46 (1H, s, imidazole ring-N-CH-; C₅), 9.05 (1H, s, imidazole ring-N-CH-N; C₂); For n-Bu₄NPF₆: 0.90 (3H, m, but-CH₃; C₄), 1.318 (2H, m, but-CH₂; C₃), 1.83 (2H, m, but-CH₂; C₂), 3.224 (2H, t, but-N-CH₂; C₁); For MeCN: 2.021 (3H, s, CH₃-CN).

Figure S9 (b). ¹H NMR (400 MHz, CDCl₃) spectrum of concentrated catholyte solution of CPBE experiment performed as per the reaction conditions given in 3rd row of Table 3: δ (ppm). No signals due to sodium formate, which appears at 9.6 ppm are seen.

2. Preparation of 0.5 M sodium phosphate (NaPi) (pH-7.4) buffer solution

The 0.5 M sodium phosphate (NaPi) (pH - 7.4) solution is a two-component buffer system in which $\text{NaH}_2\text{PO}_4 \cdot n\text{H}_2\text{O}$ is a weak acid, and its conjugate base is Na_2HPO_4 (i.e., $\text{NaHPO}_4^- + \text{H}^+$) (refer Eq. S1) with a $\text{pK}_{\text{a}2}$ value of 7.2 [1]. The Henderson-Hasselbalch equation (Eq. S2) can be used to determine when an aqueous solution of a conjugate acid/base pair is functioning as a buffer instead of a zwitterion. If the concentration of the weak acid is equal to that of its conjugate base, then the ratio of these two components is one, and in this case the Henderson-Hasselbalch equation reduces to $\text{pH} = \text{pK}_{\text{a}}$ as log of value one is equal to zero.



$$\text{pH} = \text{pK}_{\text{a}} + \log \frac{[\text{NaHPO}_4^-]}{[\text{NaH}_2\text{PO}_4]} \quad (\text{Eq. S2})$$

$$\Rightarrow 7.4 = 7.2 + \log \frac{[\text{NaHPO}_4^-]}{[\text{NaH}_2\text{PO}_4]}$$

$$\Rightarrow 0.2 = \log \frac{[\text{NaHPO}_4^-]}{[\text{NaH}_2\text{PO}_4]}$$

$$\Rightarrow \frac{[\text{NaHPO}_4^-]}{[\text{NaH}_2\text{PO}_4]} = 1.58483192; \text{ in this case } [\text{NaHPO}_4^-] = 1.58483192, \text{ whereas } [\text{NaH}_2\text{PO}_4] = 1.$$

Accordingly the decimal fractions of $[\text{NaHPO}_4^-]$ and $[\text{NaH}_2\text{PO}_4]$ as follows:

$$\Rightarrow [\text{NaHPO}_4^-] = 1.58483192 / (1.0 + 1.58483192) = 1.58483192 / 2.58483192 = 0.61313682.$$

$$\Rightarrow [\text{NaH}_2\text{PO}_4] = 1 / 2.58483192 = 0.38686318$$

In this case the molarity of ions of 0.5 M sodium phosphate (NaPi) (pH - 7.4) buffer solution can be obtained by simply multiplying the required molarity of the buffer (i.e., 0.5 M) by the decimal fraction of components, i.e., $[\text{NaH}_2\text{PO}_4]$ & $[\text{NaHPO}_4^-]$.

$$\Rightarrow \text{Moles}_{[\text{NaHPO}_4^-]} = 0.5\text{M} \times 0.61313682 = 0.3065684101 \text{ M}$$

$$\Rightarrow \text{Moles}_{[\text{NaH}_2\text{PO}_4]} = 0.5\text{M} \times 0.3868631799 = 0.19343159 \text{ M}$$

The moles of each component present in 500 mL 0.5 M sodium phosphate (NaPi) (pH-7.4) buffer solution are:

$$\Rightarrow \text{Moles of NaHPO}_4^- \text{ ions (i.e., Na}_2\text{HPO}_4) = 0.5 \text{ L} \times 0.3065684101 \text{ M/L} = 0.153284051 \text{ M}$$

$$\Rightarrow \text{Moles of NaH}_2\text{PO}_4 = 0.5 \text{ L} \times 0.19343159 \text{ M/L} = 0.096715795 \text{ M}$$

The amounts (i.e., number of grams) of NaH₂PO₄·2H₂O and Na₂HPO₄ (both are >99.5% pure SQ grade procured from Fisher-Scientific, Qualigens, Mumbai) to be dissolved in 500 mL standard volumetric flask to obtain 500 mL 0.5 M sodium phosphate (NaPi) (pH - 7.4) buffer solution are as follows:

$$\Rightarrow 0.153284051 \text{ M} \times 141.56 \text{ g/mol (i.e., the molecular weight of Na}_2\text{HPO}_4 \text{ is 141.56 g/mol)} = 21.69 \text{ grams.}$$

$$\Rightarrow 0.096715795 \text{ M} \times 156.01 \text{ g/mol (i.e., the molecular weight of NaH}_2\text{PO}_4 \cdot 2\text{H}_2\text{O is 156.01 g/mol)} = 15.088 \text{ grams.}$$

As mentioned above, the 500 mL buffer solution of 0.5 M sodium phosphate (NaPi) (pH - 7.4) was prepared by dissolving 21.69 grams Na₂HPO₄ and 15.088 grams NaH₂PO₄·2H₂O in deionized water and make-up to the mark of 500 mL standard volumetric flask.

3. Quantitative estimation of CO and H₂ gases formed in electrochemical CO₂ reduction (ECR) reaction using gas-chromatography mass-spectrometry (GC-MS) technique

Analysis of the gases formed in ECR reaction: After running CPBE experiment for about 5 min., about 0.1 mL of headspace gas from cathodic compartment was withdrawn using a de-aerated gas-tight glass-syringe (Hamilton make) through rubber septum (Suba-seal septa, Aldrich), and was injected into a gas chromatography (GC) (Agilent Technologies, 7890A, GC system, G3440A, Serial # CN10521016)-mass spectrometry (MS) (Agilent Technologies, 5975C, inert XL EI/CI MSD with Triple-Axis Detector, G3174A, Serial # US10494610) equipment fitted with a capillary column (0.530 mm × 30 m, 50 micron, -60° to 300°C, HP-MOLSIEVE, 19095P-MSO, Agilent Technologies, Inc., USA) packed with 5Å molecular sieves to separate CO, H₂, O₂ and N₂, gases using the thermal conductivity detection (TCD) method as well as mass-spectral analysis [2,3]. Contamination of the headspace by air leak was quantified

by determining the N_2 present in the headspace areas of both the compartments (using the N_2 peak on GC traces).

Determination of thermal conductivity detection (TCD) response of CO and H₂ gases: Acetonitrile (MeCN) (Chromosol V® Plus, for HPLC, >99.9%, Sigma-Aldrich) (50 mL) added with 0.1M n-Bu₄NPF₆ (≥99.0%, Sigma-Aldrich) and 50 mM bmim-BF₄ (≥97.0%, 91508-5G, Aldrich) room temperature ionic liquid (RTIL) was taken in a Teflon coated magnetic bead (almond shape) containing round bottom (RB) flask (100 mL volume) and fitted with a rubber septum (Suba-Seal® septa, Sigma-Aldrich). This RB containing solution was then fixed on a magnetic stirrer (Remi, MLH-5, Mumbai) and was degassed with an high-purity CO₂ gas (99.99%, M/s. Sicgil India (Pvt) Ltd., Chennai) from a pressure cylinder at a rate of 50 sccm for about 45 min. To this degassed solution in the RB flask, five different amounts (50 μL, 100 μL, 150 μL, 200 μL, & 250 μL) of high-purity CO gas (>99.0%, INOX Air Products Pvt. Ltd., Mumbai) from a pressure cylinder was drawn into a gas-tight syringe (10-250 μL capacity, Hamilton Syringes for GC & HPLC, Sigma-Aldrich), and injected into the solution present in the RB flask through the rubber septum. Five different amounts of CO gas were injected into the solution, and then homogenized the injected CO into the solution by stirring on a magnetic stirrer rotated at a speed of about 500 rpm for 5 min. About 50 μL head-space gas composition after injecting every different volume of CO into the solution and homogenization by stirring was drawn into the gas-tight syringe, and injected into a gas-chromatography (GC) (GC system, 7890A, Agilent Technologies, USA)-mass spectrometry (MS) (5975C inert XL EI/CI MSD with triple-axis detector, Agilent Technologies, USA) (GC-MS) instrument to identify and quantify each individual gas present in the injected gas-mixture with the help of thermal conductivity detector (TCD) and mass-spectral (MS) analysis. The same experiment was repeated for high-purity H₂ gas (>99.0%, M/s. Sicgil India (Pvt) Ltd., Chennai) also by injecting same five different amount of gas. For both CO and H₂ gases, based on the GC peaks areas generated after injecting the head-space gas mixtures, moles of gases vs. peak area plots are drawn and the resultant plot is shown in Figure S6 [2]. It is very easy to find out how many moles of CO or H₂ gas formed in the ECR reaction performed for a definite amount of time by injecting 50 μL of head-space gas-composition into GC as there is a clear-cut relationship between the moles of CO

and H₂ gases injected into GC, and the obtained GC peak area (Figure S6). It can be seen from this Figure S6 that H₂ gas has about 25 times higher response for thermal conductivity detection (TCD) than the one CO gas has. It is known that 1 μm gas occupies 22.4 μL volume at STP irrespective of the gas nature (i.e., at 0°C and 760 mmHg pressure; standard temperature and pressure). At room temperature, these gases can occupy slightly higher volumes, but these changes are ignored while calculating the faradaic efficiency (FE) values.

4. Determination of Faradaic efficiency (FE)

Eqs. S3-S5 reveals the reactions that take place on the surface of a metal cathode during electrochemical CO₂ reduction (ECR) reaction. Eq. S6 can be used to determine the Faradaic efficiency (FE) of CO + H₂ gases formed in an ECR reaction; where, $E^{\circ}_{CO_2/CO}$ is the standard reduction potential of CO₂ conversion to CO, and E is the applied potential (Table 3) [4], z is the theoretical number of electrons (e⁻) participated in reactions (Eqs. S3-S5), n is the number of moles of product(s) (CO & H₂) formed, F is the Faraday constant ($F = 96,485$ or $96,500$ Coulombs/mole (C/mole)), and q is the total charge (coulombs, C) supplied during CPBE experiment [2,5]. Each μmole CO formation needs 2 μmoles electrons (e⁻) (i.e., 0.19299 Coulombs charge) (Eqs. S3-S5), and the same is true for H₂ formation too.



$$\text{Faradaic efficiency (FE) (\%)} = \frac{z \cdot n \cdot F}{q} \times 100 \quad (S6)$$

5. Determination of number of moles of CO and H₂ gas-mixture formed in the ECR reaction in CPBE experiments

The GC analysis revealed that only 283.52 μmoles of CO and 11.81 μmoles of H₂ at a selectivity of about 91.2% and 3.8%, respectively, are formed per centimeter square area per one hour, when the CPBE experiment was performed as per the reaction conditions given in 3rd row of Table 3. These μmoles of gases accounts for the FE of about 95% [2]. 1 mole CO formation from CO₂ needs 2 moles of e⁻ (i.e., 1,93,000 Coulombs = 2 \times 96,500 Coulombs charge) as shown in Eqs. S3 & S4. One mole gas occupies 22.4 litres volume at STP. Similarly, one mole H₂ formation from H₂O also needs 2 moles of e⁻ as shown in Eq. S5. Each μmole CO formation needs 2 μmoles electrons (e⁻) (i.e., 0.193 Coulombs charge). As per the results given in the 3rd row of Table 3, about 180 Coulombs charge was passed into the ECR reaction during CPBE experiment performed for about 180 min.. If 1865 micromoles of CO + H₂ gases together are formed by consuming 180 Coulombs charge, then the Faradaic efficiency can be considered as 100%.

6. Calculation of turnover frequency (TOF)

The turnover frequency (TOF) values were calculated using formula given in Eq. S7, where, J is current density; A is the area of the electrode exposed into the electrolyte solution during reaction, F is the Faraday constant, and m is the number of moles of product (i.e., CO + H₂) formed [6]. For example, when the 3rd row of Table 3 data is considered, then the current density, $J = 27.5 \text{ mA/cm}^2$ (i.e., 27.5 mC/s/cm²) or 0.0275 C/s/cm²; when the area of the Sn cathode is considered, then $A = 1.5 \text{ cm}^2$; Faraday constant, $F = 96,500 \text{ C/mole}$; and the number of moles of CO + H₂ formed per second, $m = 0.1367 \text{ } \mu\text{moles}$ or $13.67 \times 10^{-8} \text{ moles}$).

$$\text{TOF} = \frac{J \times A}{4 \times F \times m} \quad (\text{S7})$$

7. Calculation of yield

Yield = Faradaic efficiency \times selectivity.

8. Tafel slopes generation

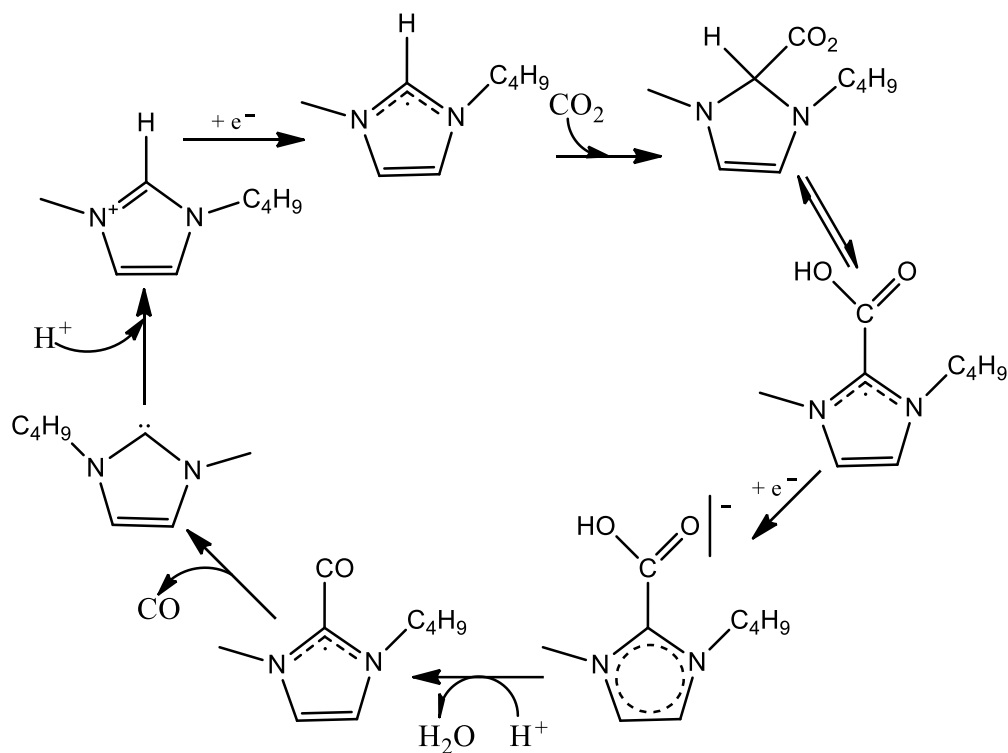
$$\text{Tafel equation } \eta = b \log (j/j_o) \quad (\text{S8})$$

The polarization curves of CVs were fitted to the Tafel equation (Eq. S8), where η is overpotential, b is the Tafel slope, j is the current density, and j_o is the exchange current density [7].

9. Calibration of reference electrode

In the CV as shown in Figure S9, the anodic and cathodic potentials of the ferrocene redox reactions are observable, it is possible to see that despite appearing ideal, upon closer inspection of the peak separation ΔE , even at a scan rate of just 20 mV s^{-1} is approximately twice the expected 59 mV for a reversible one electron transfer ($\Delta E = E_{\text{pa}} - E_{\text{pc}} \approx 130 \text{ mV}$). The number of electrons transferred is well known for this oxidation reaction therefore this deviation from ideality is attributable to uncompensated resistivity of the solvent. A similar ΔE increase has been observed by other groups working in non-aqueous solvents with an Ohmic drop often reported in non-aqueous voltammetry when compared to the more traditionally studied aqueous systems [8].

10. Supporting information Schemes, and Figures



Scheme S1. A schematic diagram showing a plausible reaction mechanism proposed by Wang *et al.* [9], that is believed to take place in an imidazolium based RTIL mediated ECR reaction to form CO in the presence of protons (H⁺) derived from water on the surface of an inert metal cathode.

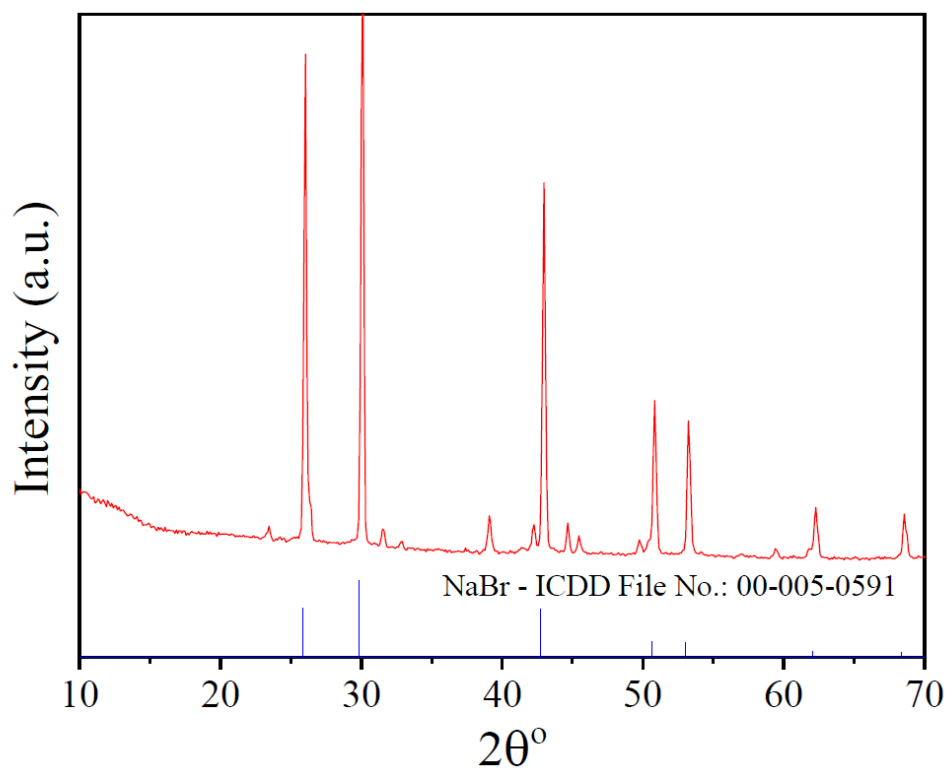


Figure S1. XRD pattern of NaBr formed as a byproduct during synthesis of bmim[BF₄] RTIL from bmim[Br] and NaBF₄ *via* metathesis reaction performed at room temperature in water medium along with ICDD file # 00-005-0591 assigned for NaBr compound.



Figure S2. A digital photograph showing the continuous liquid-liquid extraction apparatus employed for separating bmim[BF₄] RTIL from NaBr salt from the reaction mixture solution.

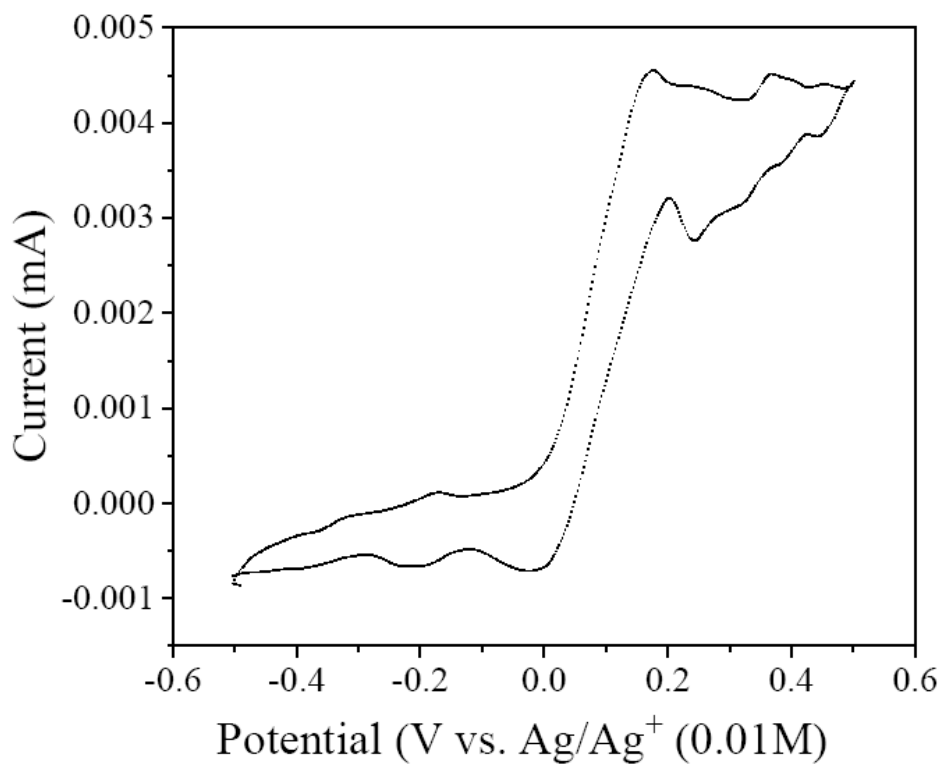


Figure S3. CV profile generated while calibrating Ag/Ag^I (0.01M) reference electrode in Ar saturated and blanketed solution of 20 mL MeCN + 200 mM n-Bu₄NPF₆ + 5 mM Ferrocene at a scan rate of 20 mV/s over Pt working (WE) and counter electrodes (CE) [8].

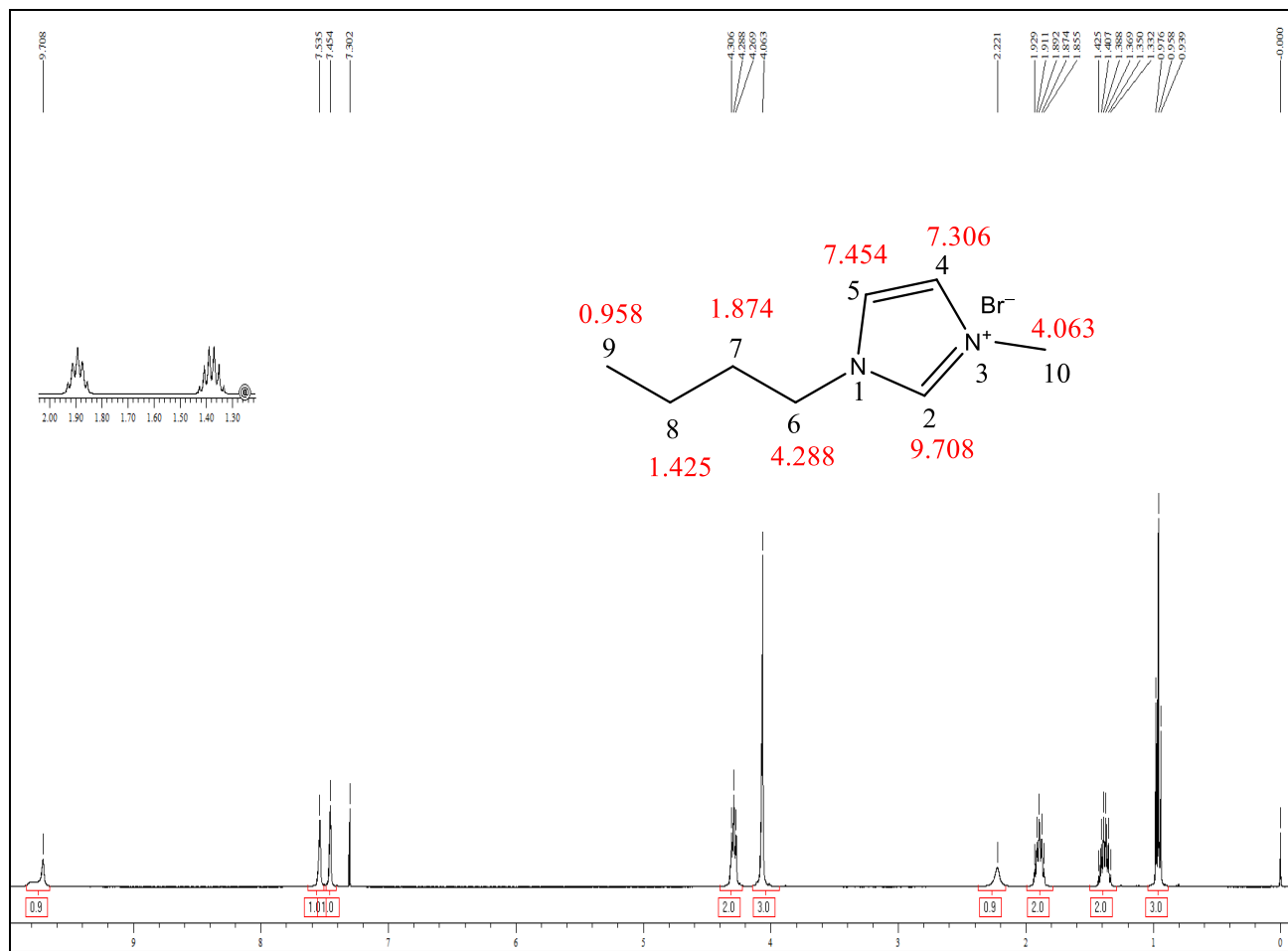


Figure S4 (a). $^1\text{H-NMR}$ spectrum of bmim[Br] RTIL synthesized in this study (refer Table 2).

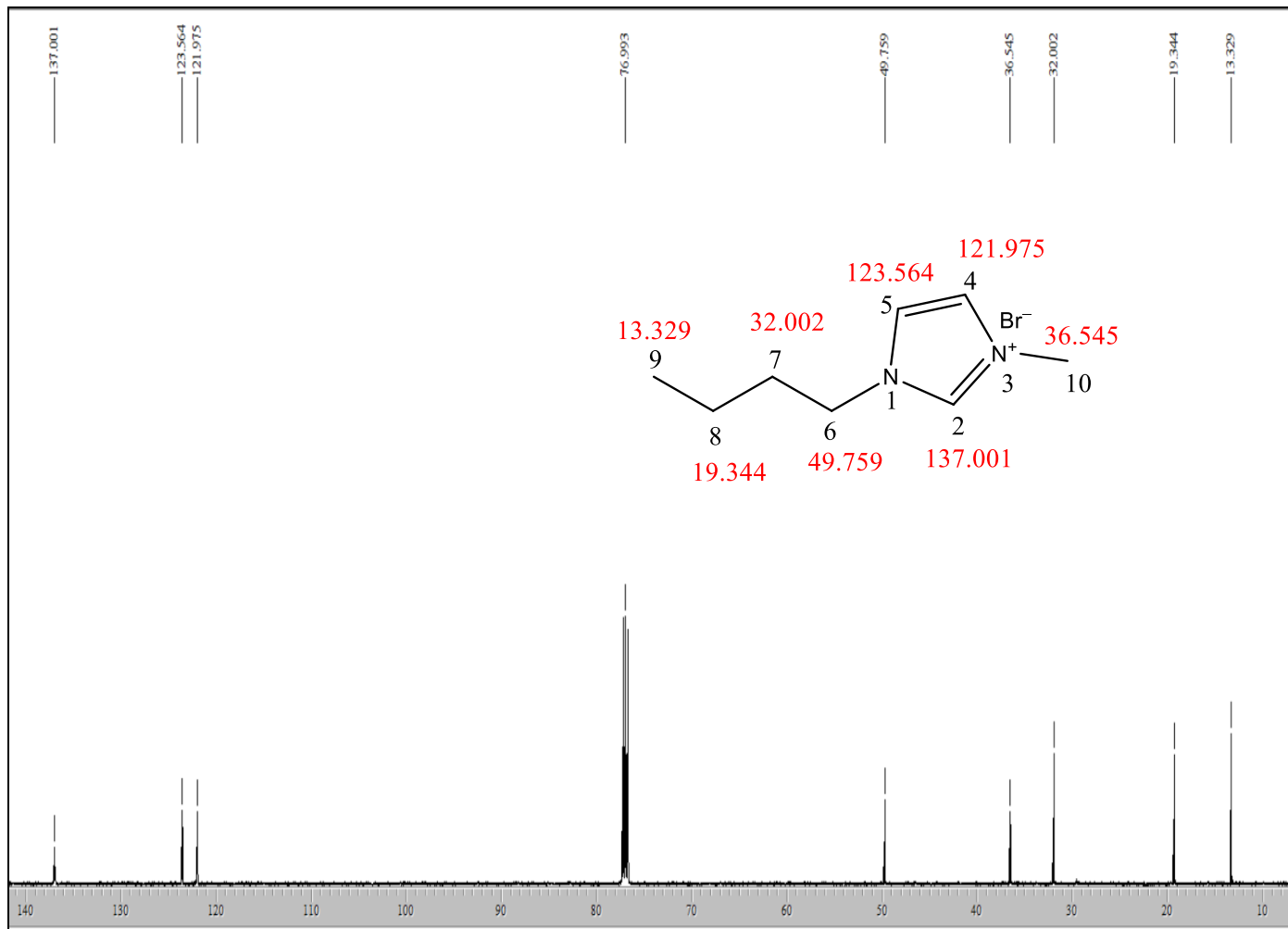


Figure S4 (b). ^{13}C -NMR (125 MHz, CDCl_3 + DMSO) spectrum of bmim[Br] compound synthesized in this study (refer Table 2).

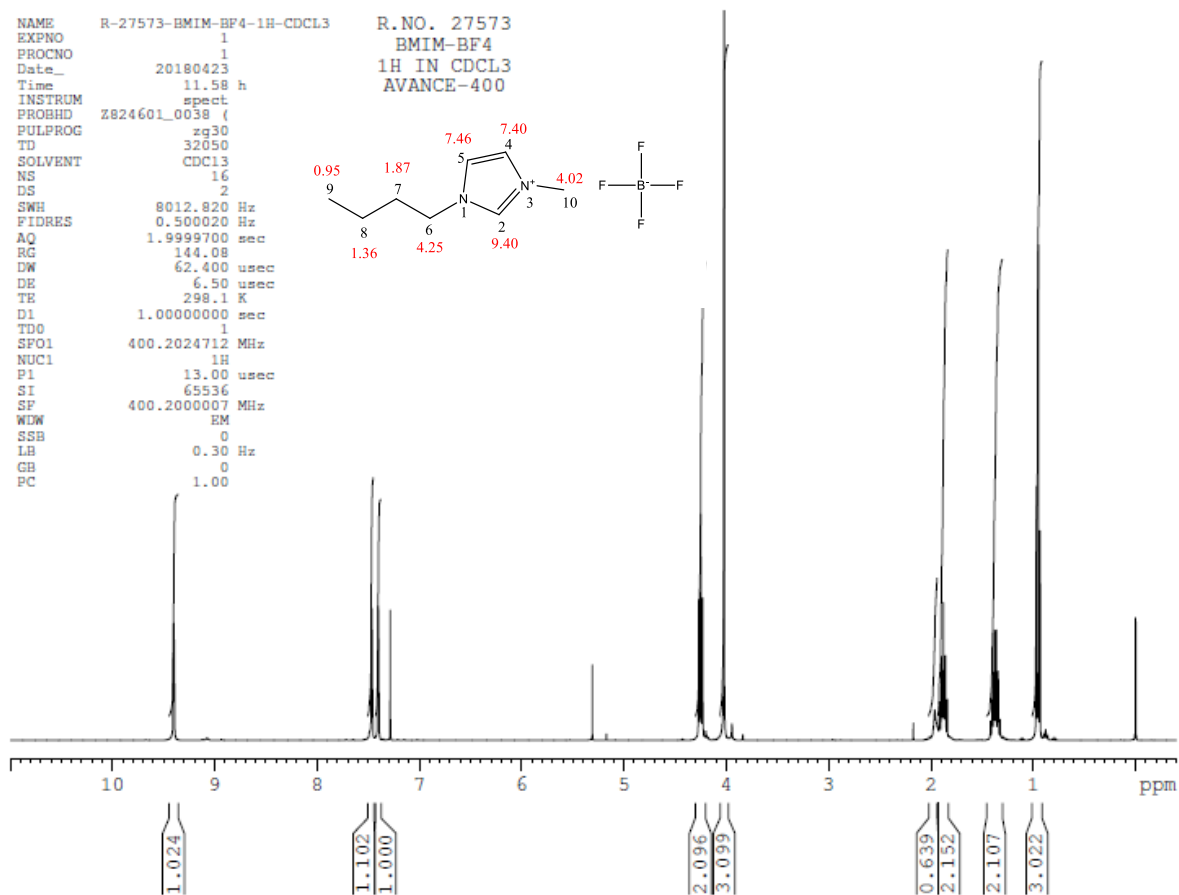


Figure S5 (a). $^1\text{H-NMR}$ of $\text{bmim}[\text{BF}_4]$ RTIL prepared in this study (refer Table 2).

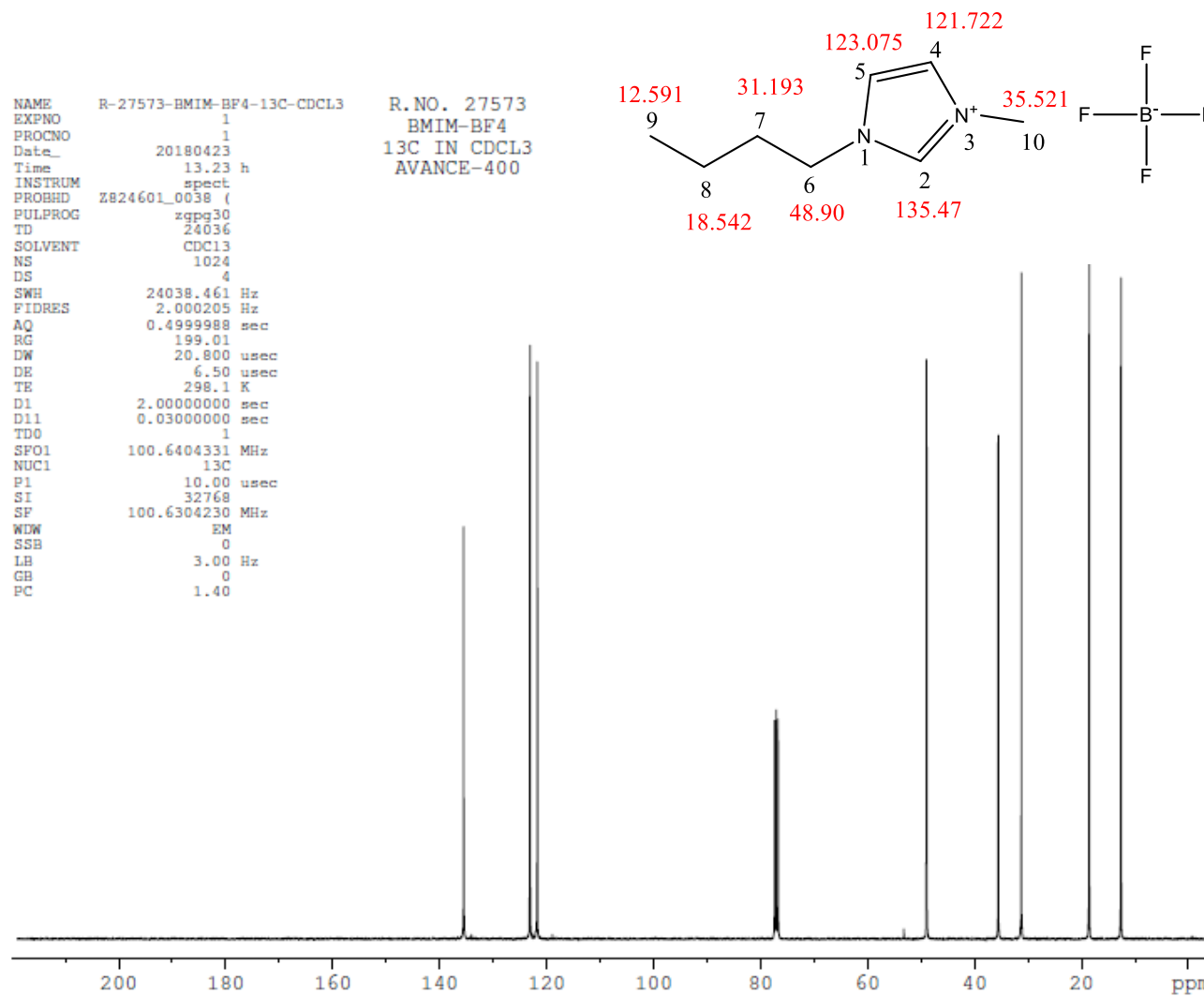


Figure S5 (b). ^{13}C -NMR (125 MHz, $\text{CDCl}_3 + \text{DMSO}$) of bmim[BF_4] RTIL prepared in this study (refer Table 2).

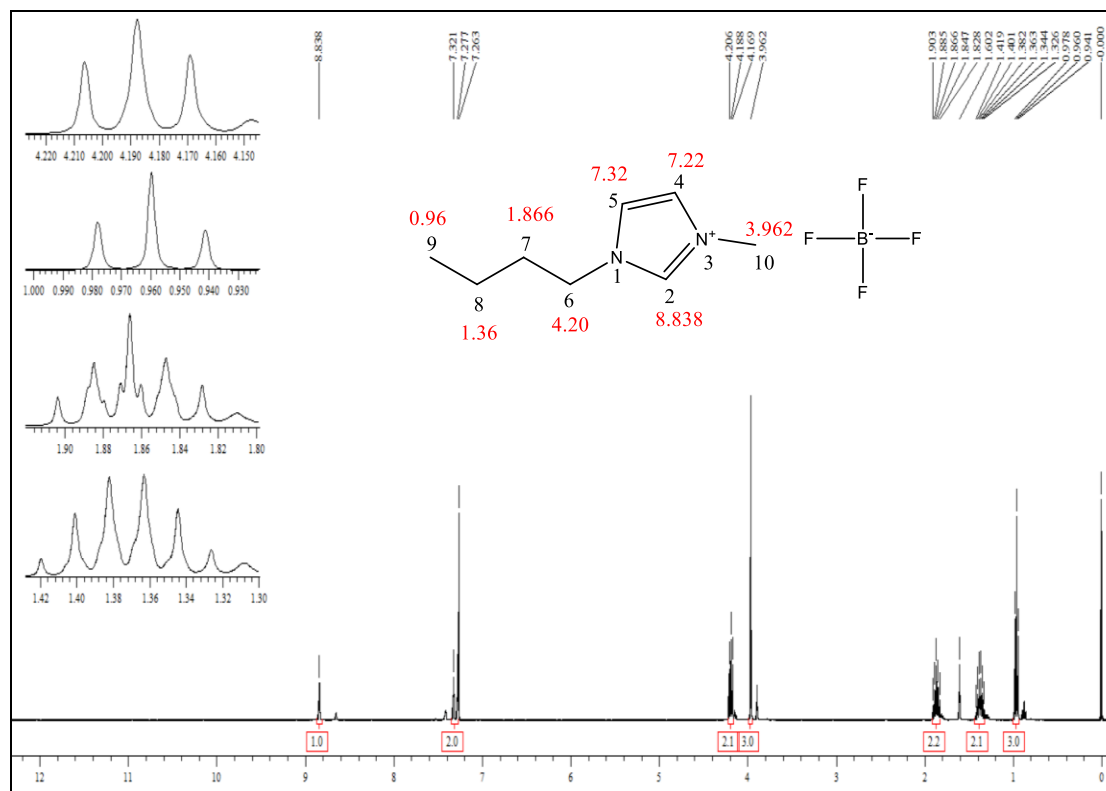


Figure S6 (a). ^1H NMR (400 MHz, CDCl_3) spectrum of bmim[BF_4] ($\geq 97.0\%$, 91508-5G) RTIL procured from Aldrich, USA (refer Table 2).

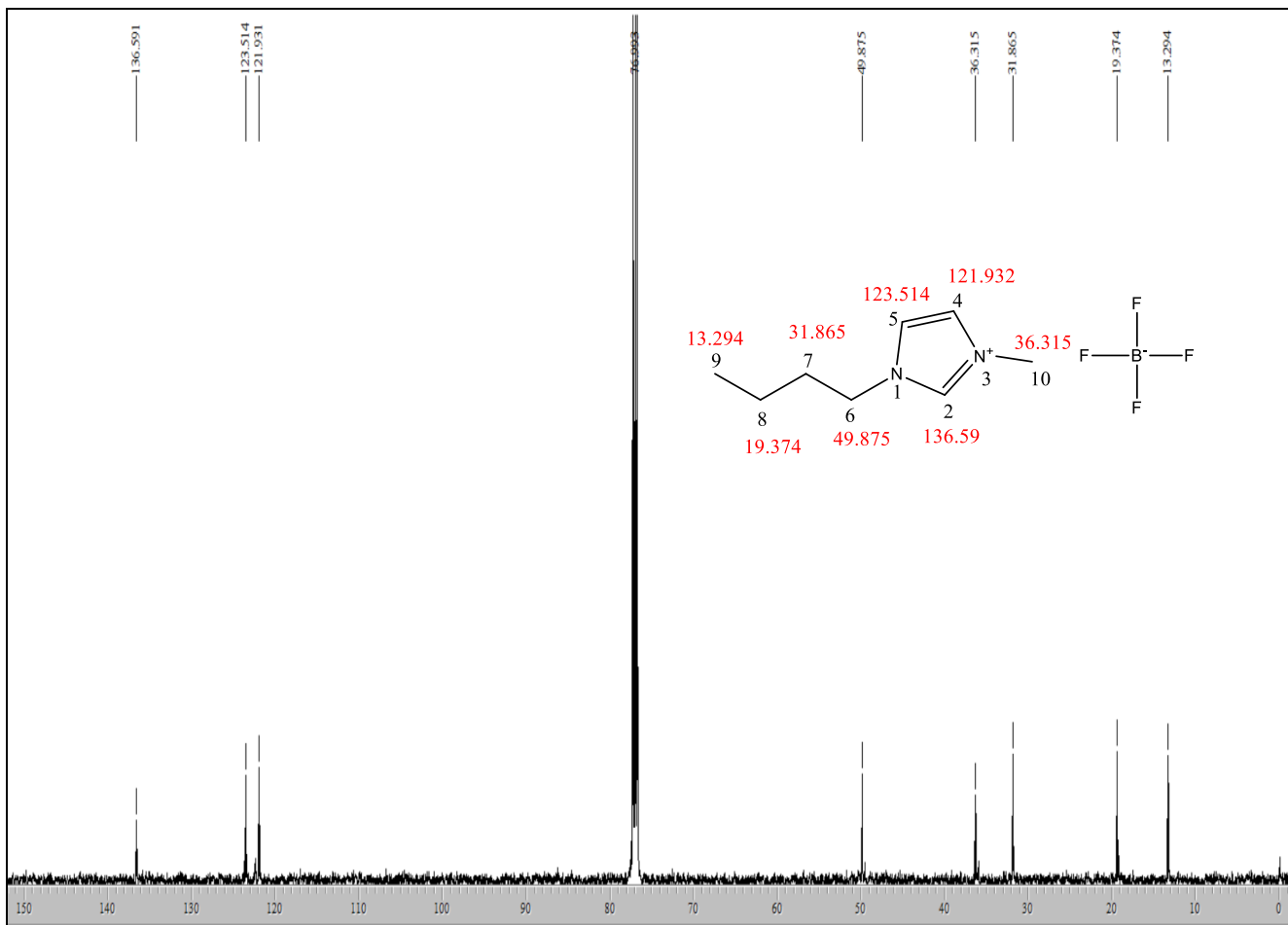


Figure S6 (b). ^{13}C -NMR spectrum of bmim[BF₄] ($\geq 97.0\%$, 91508-5G) RTIL procured from Aldrich, USA (refer Table 2).

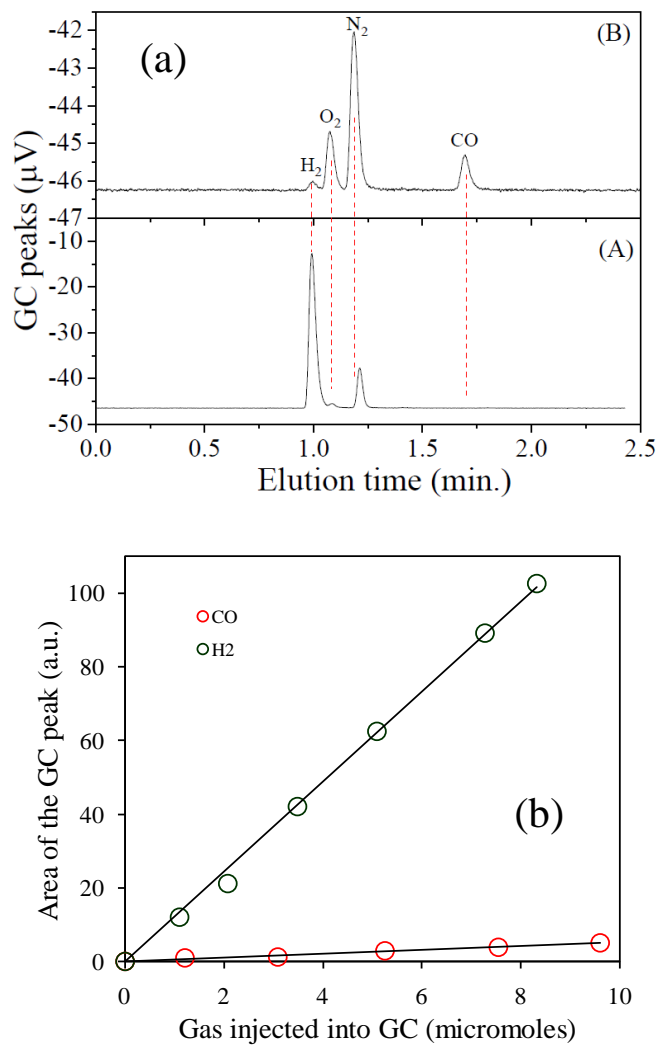


Figure S7. (a) Gas chromatograph (GC) profiles gases formed in cathodic compartment during a CPBE experiment performed as per reaction conditions given 1st and 3rd rows of Table 3, respectively; and (b) the response factors of H_2 and CO gases by thermal conductivity detector (TCD).

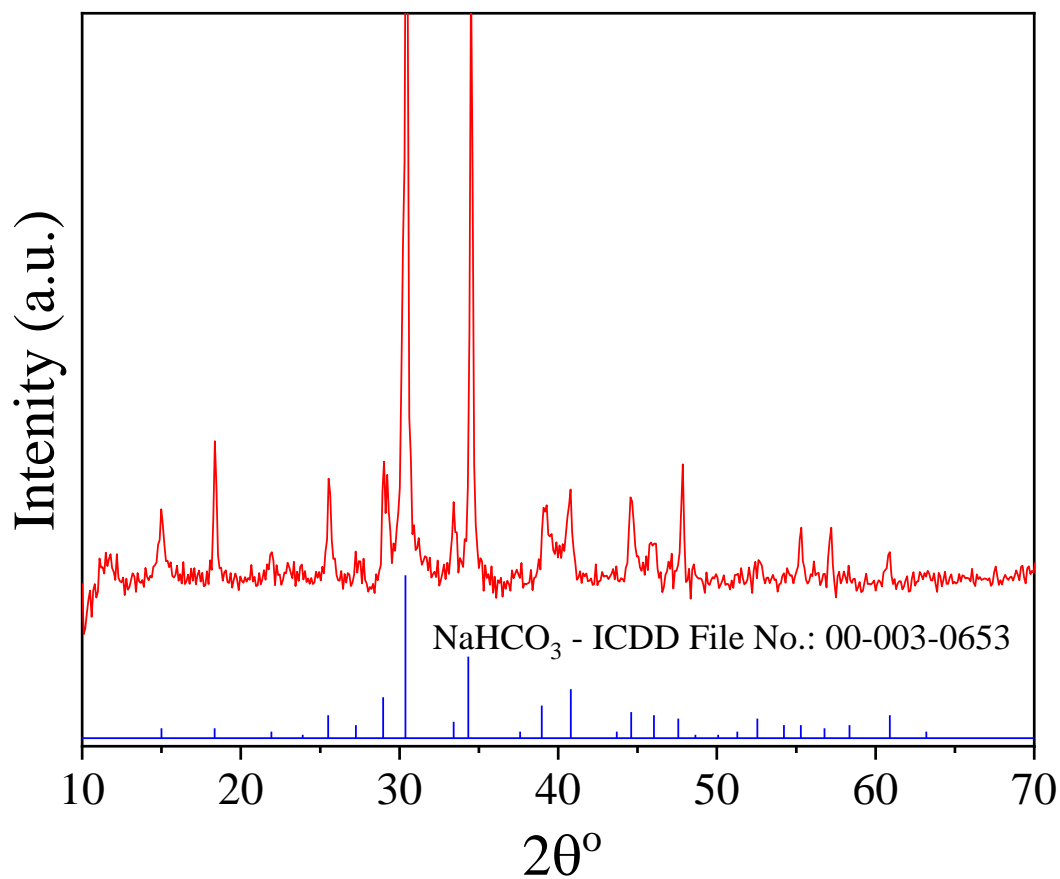


Figure S8. XRD pattern of a white precipitate *in situ* formed in the cathodic compartment during CPBE experiment conducted as per the reaction conditions given in the 3rd row of Table 3. All the major XRD peaks exhibited by this white precipitate are matching with those lines of NaHCO₃ published in ICDD File # 00-003-0653.

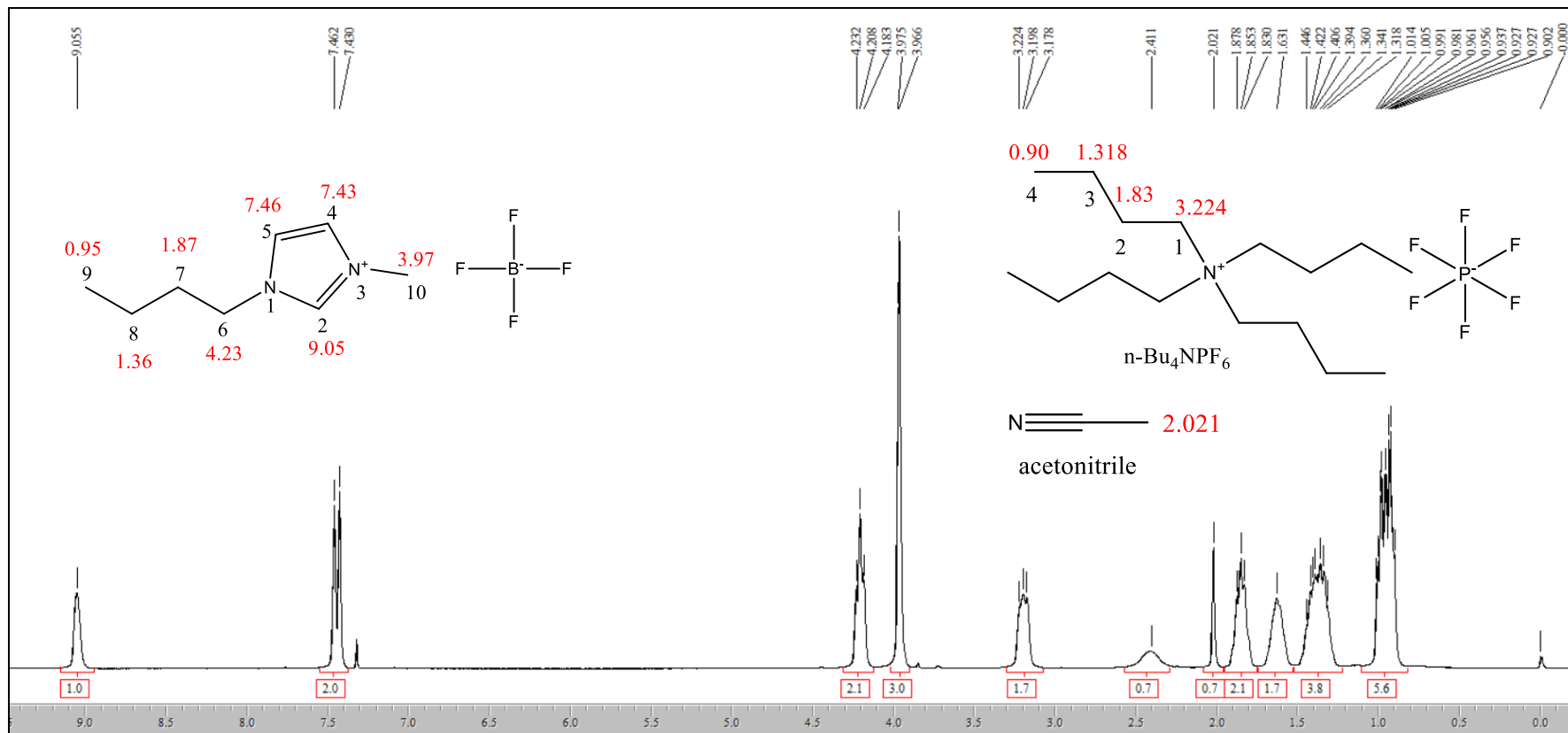


Figure S9 (a). ^1H NMR (400 MHz, CDCl_3) spectrum of concentrated catholyte solution of CPBE experiment performed as per the reaction conditions given in 3rd row of Table 3: δ (ppm) = For $\text{bmim}[\text{BF}_4]$: 0.95 (3H, m, but- CH_3 ; C $_9$), 1.36 (2H, m, but- CH_2 ; C $_8$), 1.87 (2H, m, but- CH_2 ; C $_7$), 3.97 (3H, s, N- CH_3 ; C $_{10}$), 4.23 (2H, t, but-N- CH_2 ; C $_6$), 7.43 (1H, s, imidazole ring-N- CH -; C $_4$), 7.46 (1H, s, imidazole ring-N- CH -; C $_5$), 9.05 (1H, s, imidazole ring-N- CH -N; C $_2$); For $\text{n-Bu}_4\text{NPF}_6$: 0.90 (3H, m, but- CH_3 ; C $_4$), 1.318 (2H, m, but- CH_2 ; C $_3$), 1.83 (2H, m, but- CH_2 ; C $_2$), 3.224 (2H, t, but-N- CH_2 ; C $_1$); For MeCN: 2.021 (3H, s, CH_3 -CN).

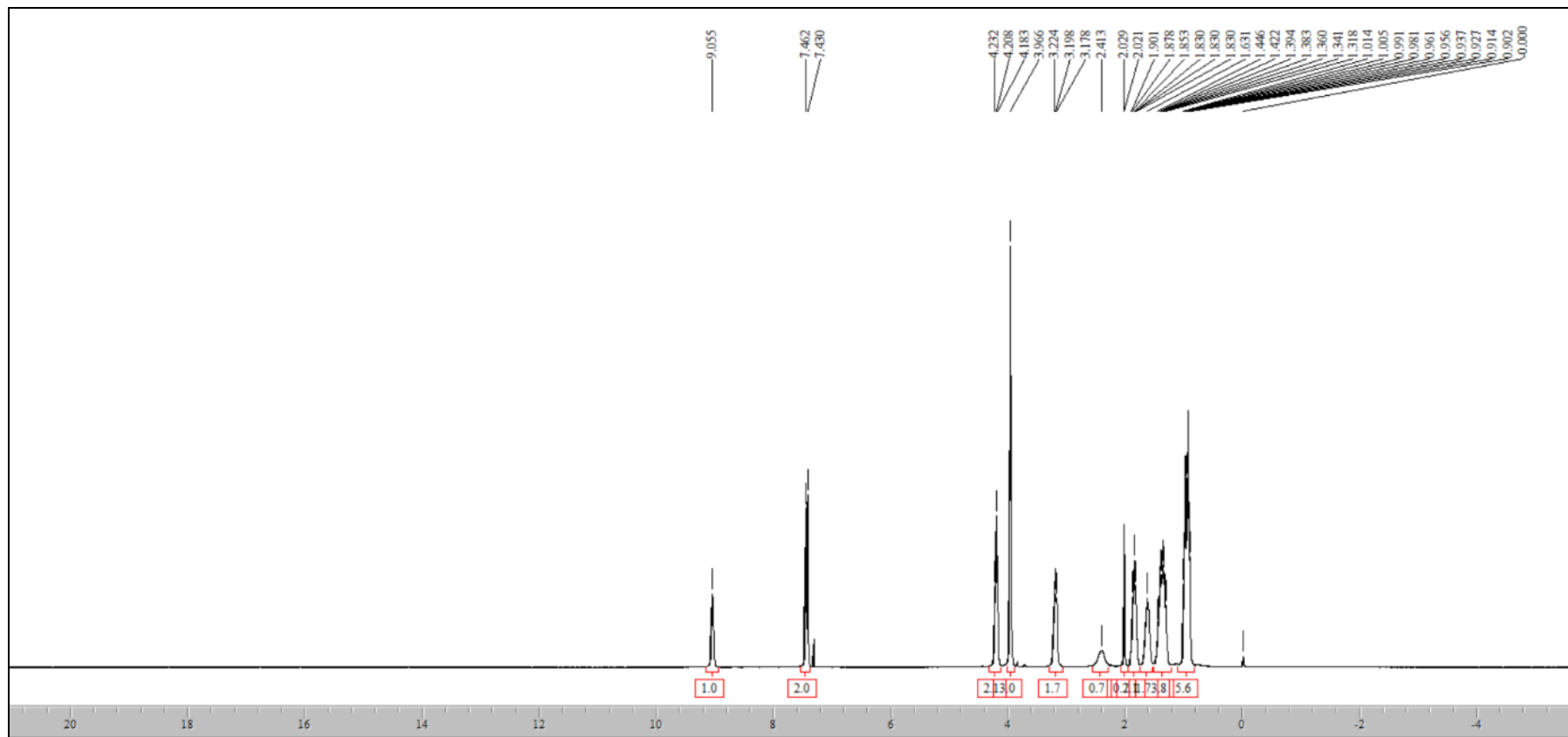


Figure S9 (b). ^1H NMR (400 MHz, CDCl_3) spectrum of concentrated catholyte solution of CPBE experiment performed as per the reaction conditions given in 3rd row of Table 3: δ (ppm). No signals due to sodium formate, which appears at 9.6 ppm are seen.

References:

- (1). <https://www.vanderbilt.edu/AnS/Chemistry/Rizzo/stuff/Buffers/buffers.html>; dated: 16th April 2019.
- (2). I. Ganesh, P. P. Kumar, I. Annapoorna, J. M. Sumliner, M. Ramakrishna, N. Y. Hebalkar, G. Padmanabham, and G. Sundararajan, *Appl. Surf. Sci.*, **293**, 229 (2014).
- (3). I. Ganesh, *Mater. Manuf. Processes*, **32**, 431 (2017).
- (4). D. T. Whipple, and P. J. A. Kenis, *J. Phy. Chem. Lett.*, **1**, 3451 (2010).
- (5). J. Albo, A. Sáez, J. S. Gullón, V. Montiel, and A. Irabien, *Appl. Catal. B: Environ.*, **176–177**, 709 (2015).
- (6). A. J. Esswein, M. J. McMurdo, P. N. Ross, A. T. Bell, and T. D. Tilley, *J. Phys. Chem. C*, **113**, 15068 (2009).
- (7). V. V. Palishchuk, and A. W. Addison, *Inorganica Chimica Acta*, **298**, 97 (2000).
- (8). A. Lewandowski, L. Waligora, and M. Galinski, Ferrocene as a Reference Redox Couple for Aprotic Ionic Liquids. *Electroanal.* **2009**, *21*, 2221-2227.
- (9). Y. Wang, M. Hatakeyama, K. Ogata, M. Wakabayashi, F. Jin, and S. Nakamura, *Physical Chem. Chem. Phy.*, **17**, 23521 (2015).